Chinese Chemical Letters 37 (2026) 111989

Contents lists available at ScienceDirect

Chinese Chemical Letters

journal homepage: www.elsevier.com/locate/cclet

Bipyridine-bridged Φ-shaped cyclo[8]thiophene[2]pyrrole: Synthesis and fluorescence properties

Yue Li[a,1], Qianyu Ding[b,c,1], Wansheng Liu[a], Yimeng Sun[a,*], Liyao Liu[a], Ye Zou[a], Yutao Cui[a,*], Jia Zhu[b,c,*], Chongan Di[a], Daoben Zhu[a,c]

[a] Beijing National Laboratory for Molecular Sciences, Key Laboratory of Organic Solids, Institute of Chemistry Chinese Academy of Sciences, Beijing 100190, China
[b] Laboratory of Theoretical and Computational Nanoscience, CAS Center for Excellence in Nanoscience, National Center for Nanoscience and Technology, Chinese Academy of Sciences, Beijing 100190, China
[c] University of Chinese Academy of Sciences, Beijing 100049, China

ARTICLE INFO

Article history:
Received 24 June 2025
Revised 16 October 2025
Accepted 20 October 2025
Available online 21 October 2025

Keywords:
Macrocycles
Oligothiophenes
CnTs
Fluorescence
AIEE

ABSTRACT

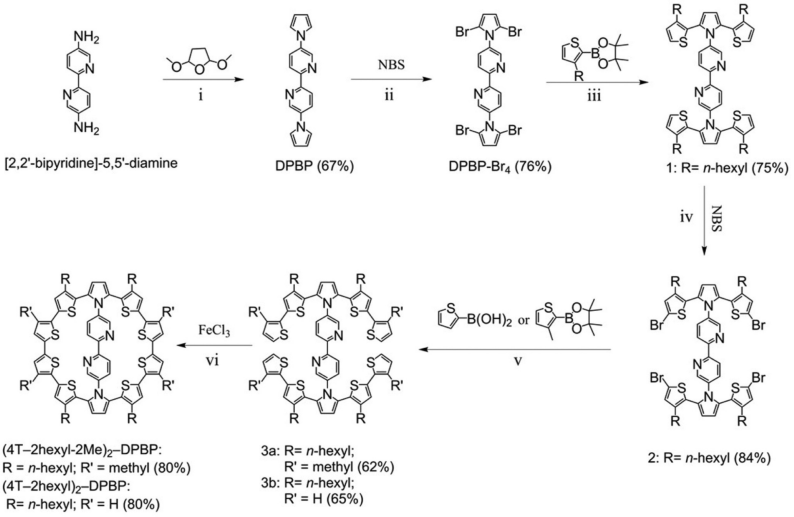
Cyclo[*n*]Thiophenes (C*n*Ts) are a distinctive class of π-conjugated macrocyclic molecules that have attracted growing attention owing to their structural aesthetics and organic electronic characteristics. However, the development of C*n*Ts has been largely impeded by inefficient synthetic route. In this work, we employ a bridge strategy using bipyridine as bridge to link two quaterthiophene units resulting in Φ-shaped bicyclosystem. This strain-retaining approach improves the synthesis efficiency of the macrocycles. Two new macrocyclic molecules, (4T-2hexyl-2Me)$_2$-DPBP and (4T-2hexyl)$_2$-DPBP, were successfully synthesized in total yield 17 % and 16 %, respectively. Single-crystal structure of (4T-2hexyl-2Me)$_2$-DPBP reveals that the bipyridine bridge is orthogonally strapped by two quaterthiophene units. Notably, both compounds exhibit aggregation-induced emission enhancement (AIEE) behavior-an unprecedented feature among C*n*T-based macrocycles. Theoretical calculations reveal that this AIE phenomenon originates from the restriction of intramolecular motion (RIM) in the aggregated state, which suppresses the non-radiative decay channels. These results demonstrate a generalized strategy for the synthesis of functional π-conjugated macrocyclic molecules based fluorescent materials.

© 2025 Published by Elsevier B.V. on behalf of Chinese Chemical Society and Institute of Materia Medica, Chinese Academy of Medical Sciences.

Macrocyclic molecules, such as cycloarenes, cyclo[*n*]paraphenylenes (CPPs), and cyclo[n]thiophenes (C*n*Ts), characterized by unique electronic properties and structural versatility, hold extensive potential applications in areas such as fluorescence, donor-acceptor interactions, global aromaticity, radical chemistry and host-guest complexes [1–7]. The study of macrocycles has been driven by their ability to mimic natural systems, such as the light-harvesting complexes in photosynthesis, and by their potential to create functional materials for optoelectronic devices. Cycloarenes and heterocloarenes, with distinctive physical structures, can serve as repeat units for nanoporous graphene, which could exploit the extended conjugated characteristic of graphene [8–10]. CPPs, a class of intriguing conjugated pure-hydrocarbon macrocycles first synthesized by Bertozzi and colleagues, have been investigated for their potential applications [11–15]. C*n*Ts are considered promising organic electronic materials in conjugated systems due to their exceptional chemical stability, optoelectronic characteristics, and charge-transport properties. Professor Peter Bäuerle and co-workers have investigated various synthesis methods for α-conjugated C*n*Ts molecules and have reported a series of C*n*Ts molecules exhibiting unique optoelectronic properties [16–20]. Considering the kinetically controlled macrocyclization reactions usually generate cyclic product mixtures leading to low yields, template-directed synthesis protocol may be a serviceable method to prepare macrocycles with high yields and functional properties. Then Professor Peter Bäuerle and co-workers developed a practical 'metal-template approach' to self-assemble bis-ethynylated building blocks and transition metal precursor complexes into stable, coordinatively bound metallamacrocycles [21,22]. Utilizing PBI as the central core, Frank Würthner and colleagues designed and synthesized cyclic (5T)$_2$-PBI and semicircle 5T-PBI, which exhibited no emission in dichloromethane (DCM) due to a rapid Förster Resonance Energy Transfer to the PBI acceptor unit [23]. Macrocycles TSP1 and TSP2, strapped by PBI, also demonstrate ultrafast electron transfer and

* Corresponding authors.
E-mail addresses: sunyimeng@iccas.ac.cn (Y. Sun), ytcui@iccas.ac.cn (Y. Cui), zhujia@nanoctr.cn (J. Zhu).
[1] These authors contributed equally to this work.

https://doi.org/10.1016/j.cclet.2025.111989
1001-8417/© 2025 Published by Elsevier B.V. on behalf of Chinese Chemical Society and Institute of Materia Medica, Chinese Academy of Medical Sciences.



Scheme 1. Synthesis route of (4T-2hexyl-2Me)$_2$-DPBP and (4T-2hexyl)$_2$-DPBP. (i) 2,5-Dimethoxytetrahydrofuran, glacial acetic acid, reflux, 24 h; (ii) NBS, THF/DCM, room temperature, overnight; (iii) Pd(PPh$_3$)$_4$, K_2CO_3, dioxane/H_2O, 120 °C, 3 days; (iv) NBS, DCM, −116 °C, overnight; (v) Pd(PPh$_3$)$_4$, K_2CO_3, dioxane/H_2O, 120 °C, 4 days; (vi) $FeCl_3$, DCM, room temperature, overnight.

sustain charge separation for an extended duration despite weak emission in DCM and DMF [24]. In summary, research on the synthetic yields and applications of functional C*n*Ts and derivatives remains limited. The key limitation for C*n*Ts and derivatives is the prevalence of ultrafast electron transfer, despite their limited conjugation within such structures.

In this work, we developed a synthetic pathway that utilized 5,5′-di(1*H*-pyrrol-1-yl)-2,2′-bipyridine (DPBP) as a bridge to link two semicircular quaterthiophene units, resulting in two bipyridine-bridged *Φ*-shaped cyclo[8]thiophenes[2]pyrrole macrocycles: (4T-2hexyl-2Me)$_2$-DPBP and (4T-2hexyl)$_2$-DPBP. Interestingly, both (4T-2hexyl-2Me)$_2$-DPBP and (4T-2hexyl)$_2$-DPBP exhibit pronounced AIEE when excited with 385 nm light in DCM/EA (ethyl acetate) solution. Aggregation-induced emission (AIE) phenomenon is one of the essential subjects concerning organic luminescent materials with a wide range of applications including biosensing, optoelectronic devices, cancer diagnosis and nanodrug delivery [25–32]. The design of conjugated AIE molecules commonly requires a suitable rotor to attenuate the energy through nonradiative transition, as well as π-conjugated portion to limit the intramolecular and intermolecular interactions to enhance the luminescence intensity and molecular aggregation state [33–37]. Despite their electronic promise, C*n*Ts and derivative molecules exhibit poor luminescence owing to the absence of conjugation and the occurrence of ultrafast electron transfer [18,23]. Compared to prior C*n*Ts and derivative molecules, our structures show a character: Symmetrically positioning an aromatic bridge (DPBP) across the ring diameter suppresses detrimental torsion, preserving conjugation and enabling AIEE phenomenon. C10Ts commonly possess planar conformation and the cycle diameter is commensurate with the dimensions of bipyridine. In both bipyridine bridged macrocycles, the rotation of the thiophene modules is intriguingly constrained by the optimally sized DPBP bridge. By straddling two semicircular quaterthiophene units, the dihedral angle between the thiophene arms is effectively fixed, enabling AIEE behavior in both macrocycles. We here reported the first observation of AIEE phenomenon in C*n*Ts and derivatives, which may open avenues for functionalizing C*n*Ts and derivatives in biomedicine and optoelectronics.

Macrocycles (4T-2hexyl-2Me)$_2$-DPBP and (4T-2hexyl)$_2$-DPBP were successfully synthesized through a series of reactions from commercial starting material [2,2′-bipyridine]−5,5′-diamine, including Paal Knorr, Wohl-Ziegler, Suzuki coupling, and Scholl reactions in commendable total yields of 17 % and 16 % (Scheme 1). Our stepwise synthesis strategy referred to the previously reported synthesis methods for macrocyclic molecules which may be adapted to relevant synthesis with more functional groups and ideal yields [23,24,38,39]. Details can be found in Supporting information. [2,2′-Bipyridine]−5,5′-diamine and 2,5-dimethoxytetrahydrofuran were dissolved in glacial acetic acid and heated to reflux, obtaining DPBP with a yield of 67 %. DPBP and *N*-bromosuccinimide (NBS) were dissolved in a component solvent of DCM and THF at ambient temperature, yielding DPBP-Br$_4$ with a 76 % efficiency. Suzuki coupling reactions of DPBP-Br$_4$ with 2-(3-hexylthiophen-2-yl)-4,4,5,5-tetramethyl-1,3,2-dioxaborolane facilitated by K_2CO_3 and Pd(PPh$_3$)$_4$, produced compound **1** (75 %). Furthermore, the room temperature reaction of NBS with **1** yielded compound **2** (84 %). Another Suzuki coupling reaction of compound **2** with either 2-thiopheneyl boronic acid or 4,4,5,5-tetramethyl-2-(3-methylthiophen-2-yl)-1,3,2-dioxaborolane, conducted at 120 °C, yielded **3a** (65 %) and **3b** (62 %). $FeCl_3$ was used to oxidize **3a** and **3b**, obtaining (4T-2hexyl-2Me)$_2$-DPBP in an 80 % yield and (4T-2hexyl)$_2$-DPBP in an 80 % yield. All the synthesized intermediates and products were characterized by ^{1}H and ^{13}C NMR spectroscopy and high-resolution mass spectrometry. ^{1}H NMR spectroscopy (Fig. 1) revealed distinct differences between **3a** and (4T-2hexyl-2Me)$_2$-DPBP. The DPBP moiety in both **3a** and (4T-2hexyl-2Me)$_2$-DPBP is flanked by two half-oligothiophene rings, while the H atoms of bipyridyl moiety exhibit similar peaks in ^{1}H NMR spectra. The disappearance of the d peak at the g site in **3a**, along with the transformation of the d peak at f positions in **3a** transforms into a singlet peak in (4T-2hexyl-2Me)$_2$-DPBP, confirms the formation of (4T-2hexyl-2Me)$_2$-DPBP and its high symmetry. Analogous spectral changes are observed in the ^{1}H NMR spectra of **3b** and (4T-2hexyl)$_2$-DPBP. The disappearance of the standard dd peak at the g site in **3b** implies the successful synthesis of (4T-2hexyl)$_2$-DPBP. The thermogravimetric analysis (TGA) indicates that the decomposition temperature of both (4T-2hexyl-2Me)$_2$-DPBP and (4T-2hexyl)$_2$-DPBP is above 300 °C. To better understand the synthesis process and the absolute structure, single crystals suitable for X-ray diffraction analysis were grown. Single crystals of **3a**, obtained by recrystallization from ethanol, were yellow block crystals and belonged to the *P*-1 space group of the triclinic system. Unexpectedly, the thiophene groups did not form a *quasi*-ring in

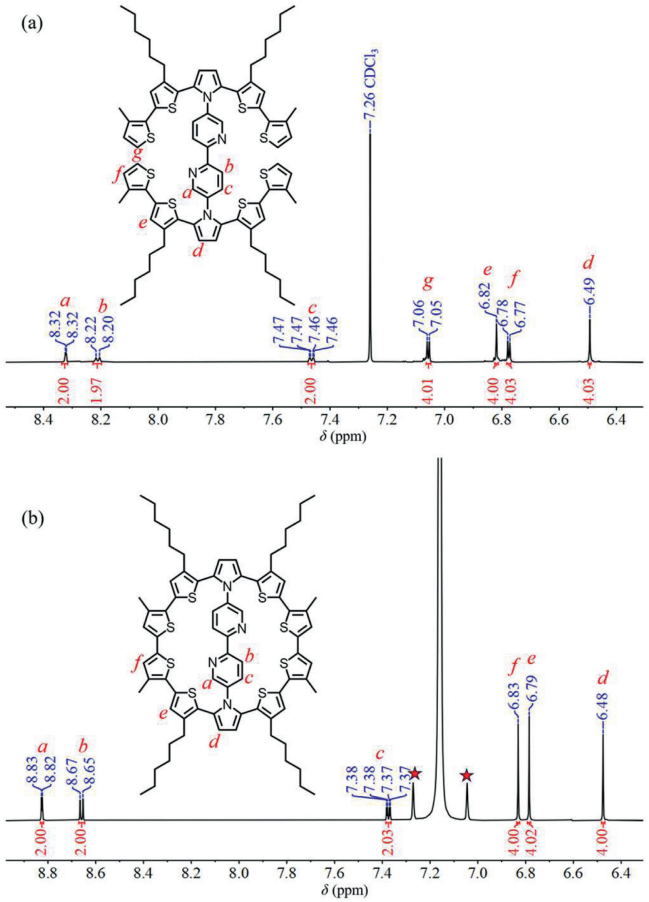


Fig. 1. ^{1}H NMR spectra of (a) **3a** in $CDCl_3$ and (b) (4T-2hexyl-2Me)$_2$-DPBP in C_6D_6.

crystals, while the ^{1}H NMR spectrum indicated a high degree of symmetry in solution. These observations strongly suggest that the macrocycle-closing reaction occurs in the solution rather than the solid state.

Single crystal (4T-2hexyl-2Me)$_2$-DPBP was grown by the diffusion of methanol into a solution of (4T-2hexyl-2Me)$_2$-DPBP in trichloromethane. (4T-2hexyl-2Me)$_2$-DPBP crystallizes in the monoclinic space group *C*2/*m*, with a quarter of (4T-2hexyl-2Me)$_2$-DPBP molecules in the asymmetric unit. The symmetry of space group *C*2/m is higher than the triclinic *P*-1 in TSP2 and (5T)$_2$-PBI. As shown in Fig. 2, the 2,2′-bipyridine group is located in the mirror plane and perpendicular to the plane of the thiophene ring. Additionally, the 2-fold axes perpendicular to the mirror plane pass through the center of the 2,2′-bipyridine group. Two adjacent methylthiophenyl groups are almost coplanar, with a small twist angle of 0.9°. The neighboring methylthiophenyl and hexylthiophenyl groups exhibit a torsion angle of 30.0°, while hexylthiophenyl and pyrrole groups exhibit a torsion angle of 35.0°. The slight rotation of hexylthiophenyl and pyrrole groups, acting as rotors, allows the overall structure to emit fluorescence. The nearest neighbor (4T-2hexyl-2Me)$_2$-DPBP macrocycles are connected by relatively weak C–H···π (3.92 Å) interactions, which may have a minor effect on their slight rotation and enhance the conjugation in the rigid macrocycles. The C–H···π interactions are weak and the distance (4.47 Å) between thiophene groups in adjacent molecules exceeds the distance typically associated with $\pi\cdots\pi$ interactions, which may be derived from the steric effect from orthogonal bipyridine groups. Meanwhile, the ^{1}H NMR also reveals that (4T-2hexyl-2Me)$_2$-DPBP exhibits a high degree of symmetry in solution compared to the reported structures [23,24]. These findings indicate that (4T-2hexyl-2Me)$_2$-DPBP manifests a similar conjugated rigid structure in both solid and solution states.

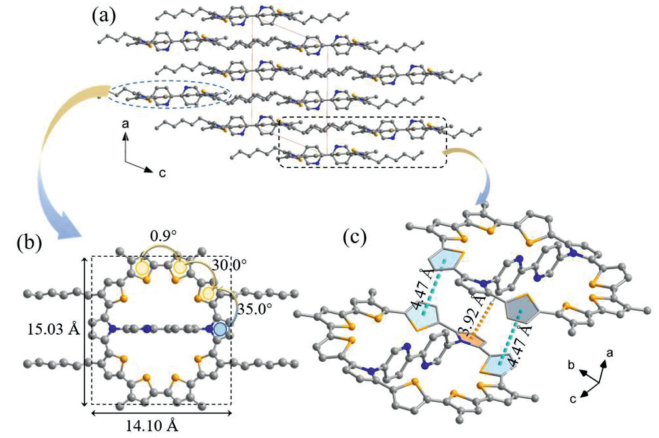


Fig. 2. (a) Crystal structure of (4T-2hexyl-2Me)$_2$-DPBP as seen from *b* axis. (b) Molecular structure of (4T-2hexyl-2Me)$_2$-DPBP. (c) The C–H···π interactions and the distance of thiophene groups in adjacent molecules. The hydrogen atoms, solvent molecules as well as the partial alkyl chains are omitted for clarity.

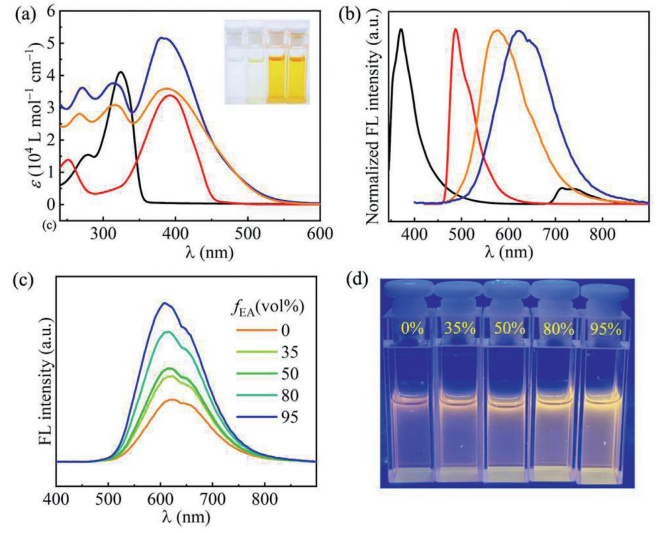


Fig. 3. (a) UV–vis absorption spectra ($c_0 = 5 \times 10^{-5}$ mol/L) and (b) normalized fluorescence emission spectra of DPBP (black), α−4T (red), (4T-2hexyl-2Me)$_2$-DPBP (blue), and (4T-2hexyl)$_2$-DPBP (orange) dissolved in DCM. Inset: Photograph of DPBP, α−4T, (4T-2hexyl-2Me)$_2$-DPBP, and (4T-2hexyl)$_2$-DPBP (left to right) in natural light. (c) Emission spectra of (4T-2hexyl-2Me)$_2$-DPBP with the excitation wavelengths $\lambda_{ex} = 385$ nm. (d) Photograph of (4T-2hexyl-2Me)$_2$-DPBP in DCM/EA system under 365 nm UV light.

To explore the characteristics of (4T-2hexyl-2Me)$_2$-DPBP and (4T-2hexyl)$_2$-DPBP, UV–vis absorption spectroscopy and steady-state emission spectroscopy were performed on DPBP, α−4T (2,2′:5′,2″:5″,2‴-quaterthiophene), (4T-2hexyl-2Me)$_2$-DPBP, and (4T-2hexyl)$_2$-DPBP as shown in Fig. 3a. Compared to the π-π^* transition of α−4T and DPBP components, (4T-2hexyl-2Me)$_2$-DPBP and (4T-2hexyl)$_2$-DPBP exhibit distinct vibronic fine structure in the higher energy region of UV–vis spectrum. The absorption spectrum of (4T-2hexyl-2Me)$_2$-DPBP shows three maximum absorption peaks at 385 nm ($\varepsilon = 51{,}485$ L mol^{-1} cm^{-1}), 313 nm ($\varepsilon = 37{,}598$ L mol^{-1} cm^{-1}) and 270 nm ($\varepsilon = 36{,}218$ L mol^{-1} cm^{-1}) in the 250–550 nm range. Similarly, (4T-2hexyl)$_2$-DPBP exhibits three absorption peaks at 388 nm ($\varepsilon = 35{,}997$ L mol^{-1} cm^{-1}), 316 nm ($\varepsilon = 30{,}847$ L mol^{-1} cm^{-1}) and 267 nm ($\varepsilon = 28{,}033$ L mol^{-1} cm^{-1}) within the same absorption range. Compared to the α−4T, the maximum absorption peaks of (4T-2hexyl-2Me)$_2$-DPBP and (4T-

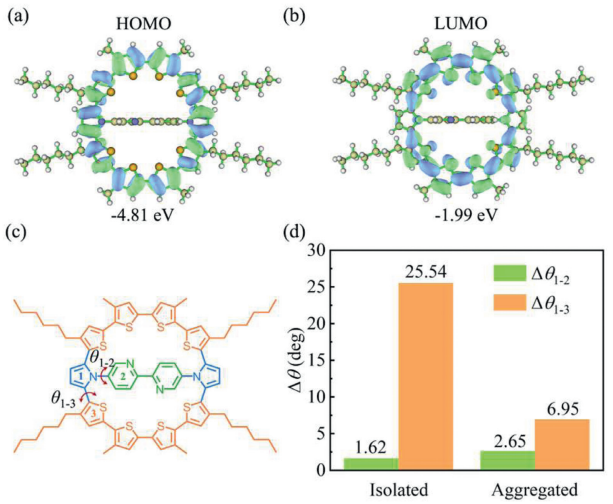


Fig. 4. Theoretical investigation on the AIE mechanism of (4T-2hexyl-2Me)$_2$ -DPBP. (a) HOMO (left) and LUMO (right) of (4T-2hexyl-2Me)$_2$-DPBP at S_0 state. (b) Scheme of selected dihedral angles θ_{1-2} and θ_{1-3}. The angle θ_{1-2} represents the dihedral angle between the pyrrole and bipyridine group, while θ_{1-3} describes the planarity of the thiophene ring (*i.e.*, the dihedral angle between the pyrrole and the adjacent thiophene). (c) Comparison of the changes in dihedral angles $\Delta\theta$ from S_0 to S_1 between the isolated and aggregated states.

2hexyl)$_2$-DPBP are blue-shifted by 7 nm and 4 nm, respectively, indicating both 4T-bridges remain in conjugation, which is consistent with the ^{1}H NMR spectrum and single crystal structure.

Normalized fluorescence emission spectra of DPBP ($\lambda_{ex}=325$ nm), $\alpha-4T$ ($\lambda_{ex}=400$ nm), (4T-2hexyl-2Me)$_2$-DPBP ($\lambda_{ex}=385$ nm), and (4T-2hexyl)$_2$-DPBP ($\lambda_{ex}=385$ nm) in DCM were recorded (Fig. 3b), which indicates that both (4T-2hexyl-2Me)$_2$-DPBP and (4T-2hexyl)$_2$-DPBP show red-shifts compared with DPBP and $\alpha-4T$ The maximum emission peaks of DPBP, $\alpha-4T$, (4T-2hexyl-2Me)$_2$-DPBP, and (4T-2hexyl)$_2$-DPBP are 375, 500, 635, and 585 nm, respectively, which indicates the fluorescence emission of (4T-2hexyl-2Me)$_2$-DPBP and (4T-2hexyl)$_2$-DPBP mainly originate from the thiophene rings. The solid-state fluorescence of both (4T-2hexyl-2Me)$_2$-DPBP and (4T-2hexyl)$_2$-DPBP exhibit similar fluorescence emission peaks with liquid state. DCM was used as the benign solvent to investigate the fluorescence behavior of (4T-2hexyl-2Me)$_2$-DPBP and (4T-2hexyl)$_2$-DPBP. When 4T-(2hexyl-2Me)$_2$-DPBP in DCM was excited by 385 nm light, it exhibited a fluorescence emission peak at 500–800 nm. When poor solvent EA was added to the DCM solution, the mixture exhibited distinct yellow emission. As the f_{EA} was further increased, the FL was significantly enhanced (Figs. 3c and d). The emission intensity of the maximum peak at 620 nm increased monotonically as the f_{EA} was increased from 0 % to 95 %, which can be attributed to the aggregation-enhanced emission resulting from the restriction of molecular motion with the increased intermolecular C–H···π interactions. The restricted rotation of the thienyl group also leads to a slight blue shift in the emission [40–42]. Transmission Electron microscopy (TEM) and dynamic light scattering (DLS) results can indicate both (4T-2hexyl-2Me)$_2$-DPBP and (4T-2hexyl)$_2$-DPBP have undergone aggregation, as shown in Figs. S21, S22, S27 and S28 (Supporting informaion).

To elucidate the mechanism of AIE generation, density functional theory (DFT) calculations were performed based on the crystal structure (Fig. 4). At both the S_0 and S_1 optimized geometries (Figs. S29-S31 in Supporting information), the highest occupied molecular orbital (HOMO) and the lowest unoccupied molecular orbital (LUMO) of (4T-2hexyl-2Me)$_2$-DPBP are delocalized across the macrocyclic composed of the thiophene and pyrrole groups (overlap index = 0.74 at S_1 state), indicating a negligible intramolecular charge transfer (ICT) contribution [43–46] and a dominant π-π^* transition over the conjugated structure upon photoexcitation [47].

Table 1
Dihedral angles θ_{1-2} and θ_{1-3} at the S_0 and S_1 minimum and reorganization energies λ in the isolated and aggregated states.

Parameter	The isolated state			The aggregated state		
	S_0	S_1	$\lvert\Delta(S_1\text{-}S_0)\rvert$	S_0	S_1	$\lvert\Delta(S_1\text{-}S_0)\rvert$
θ_{1-3} (deg)	−91.67	−90.05	1.62	−91.50	−88.85	2.65
θ_{1-2} (deg)	−50.10	−24.56	25.54	−37.88	−30.93	6.95
λ (eV)		0.93			0.47	

Further investigation into the geometric relaxation upon $S_0 \rightarrow S_1$ excitation reveals that the thiophene-pyrrole dihedral angle deviation $\Delta\theta_{1-3}$ decreases from 25.54° in the isolated state to 6.95° in the aggregated state, while the dihedral angle θ_{1-2} of the bipyridine group and the thiophene ring shows minimal variation ($\Delta\theta_{1-2,isolated}=1.62°$, $\Delta\theta_{1-2,aggregated}=2.65°$) as shown in Figs. 4b and c. This directly visualizes the restriction of thiophene ring rotation in the aggregated state. To quantify the energetic consequences of this structural relaxation, we evaluated the reorganization energy (λ) [48]. As shown in Table 1, the value of λ decreased from 0.93 eV to 0.47 eV with the occurrence of aggregation, indicating that the energy dissipation pathway dependent on molecular conformational changes is effectively suppressed. Therefore, we attribute the AIE phenomenon to the restriction of intramolecular motion (RIM) in the aggregated state, which effectively blocks the non-radiative decay pathway associated with conformational changes and is consistent with the observed fluorescence enhancement [49–54].

Fluorescence lifetime and quantum yields of (4T-2hexyl-2Me)$_2$-DPBP and (4T-2hexyl)$_2$-DPBP were investigated in DCM/EA mixtures with varying volume fractions. Both (4T-2hexyl-2Me)$_2$-DPBP and (4T-2hexyl)$_2$-DPBP exhibit photoluminescence under 385 nm UV irradiation, which is attributed to their conjugated structures. The average lifetime of both (4T-2hexyl-2Me)$_2$-DPBP and (4T-2hexyl)$_2$-DPBP are the nanosecond level (*e.g.*, 0.761 ns for $f_{EA}=95$ %, (4T-2hexyl-2Me)$_2$-DPBP, Table S3 in Supporting information), suggesting that their emission bands originate from S_1 state. Furthermore, as the f_{EA} increases, the average lifetime of (4T-2hexyl-2Me)$_2$-DPBP and (4T-2hexyl)$_2$-DPBP increases from 613.4 ps to 761.5 ps and from 577.2 ps to 751.7 ps, respectively. These results are consistent with those previously reported AIE characteristics [55–58]. The quantum yields of (4T-2hexyl-2Me)$_2$-DPBP and (4T-2hexyl)$_2$-DPBP in DCM were 0.15 % and 0.41 %, respectively. Upon the addition of EA, the quantum yields gradually increased to 2.47 % and 1.00 %, respectively.

In conclusion, we successfully synthesized two rigid Φ-shaped cyclo[8]thiophenes[2]pyrrole macrocyclic molecules, (4T-2hexyl-2Me)$_2$-DPBP and (4T-2hexyl)$_2$-DPBP, *via* a rationally designed strain-retaining bridge macrocyclization strategy. The macrocycles were obtained in moderate total yields of 17 % and 16 %, respectively. The incorporation of a bipyridine bridge not only improves the synthetic efficiency but also imparts the macrocycles with high symmetry and planar π-conjugation. Notably, both (4T-2hexyl-2Me)$_2$-DPBP and (4T-2hexyl)$_2$-DPBP exhibit aggregation-induced emission enhancement (AIEE)-a rare feature among C*n*T-based macrocyclic molecules, which we attribute to the intermolecular C–H···π interaction in the aggregated state. DFT calculations also indicate that the AIE phenomenon results from the RIM mechanism in the aggregated state. Although the fluorescence lifetimes are shorter than those of conventional AIE-active materials, this behavior is unprecedented within the C*n*Ts and high-

lights a new functional potential for such macrocyclic systems. Macrocyclic structures with AIEE properties could become high-temperature-resistant fluorescent imaging materials, optoelectronic devices. Overall, our findings provide a generalized approach for constructing π-conjugated macrocycles and represent a significant step toward developing functional organic materials with tunable optoelectronic properties.

Declaration of competing interest

The authors declare that they have no known competing financial interests or personal relationships that could have appeared to influence the work reported in this paper.

CRediT authorship contribution statement

Yue Li: Writing – original draft, Visualization, Project administration, Investigation, Formal analysis, Data curation, Conceptualization. **Qianyu Ding:** Writing – original draft, Visualization, Project administration, Investigation, Formal analysis, Data curation, Conceptualization. **Wansheng Liu:** Investigation, Data curation. **Yimeng Sun:** Writing – review & editing, Writing – original draft, Supervision, Methodology, Data curation. **Liyao Liu:** Investigation. **Ye Zou:** Investigation. **Yutao Cui:** Writing – review & editing, Writing – original draft, Supervision, Methodology, Data curation. **Jia Zhu:** Writing – review & editing, Writing – original draft, Supervision, Software. **Chongan Di:** Writing – review & editing. **Daoben Zhu:** Writing – review & editing.

Acknowledgments

The authors acknowledge the financial support from the Strategic Priority Research Program of the Chinese Academy of Sciences (No. XDB0520000), the National Key R&D Program of China (No. 2022YFA1203200), National Natural Science Foundation of China (No. 52273170), the Youth Innovation Promotion Association of the Chinese Academy of Sciences (No. 2021030), Postdoctoral Fellowship Program of CPSF (No. GZC20232735), and BMS Junior Fellow of Beijing National Laboratory For molecular Science (No. 2023BMS20111). We thank Dr. Hao Wei from Zhejiang University for his help in the theoretical calculations.

Supplementary materials

Supplementary material associated with this article can be found, in the online version, at doi:10.1016/j.cclet.2025.111989.

References

[1] N. Zhang, L.F. Yang, W.H. Li, et al., J. Am. Chem. Soc. 144 (2022) 21521–21529.
[2] X.N. Sun, A. Liu, K. Xu, et al., Aggregate 5 (2024) e607.
[3] T. Terabayashi, E. Kayahara, Y. Zhang, et al., Angew. Chem. Int. Ed. 62 (2022) e202214960.
[4] T. Ide, W.C. Huang, M. Horie, J. Am. Chem. Soc. 146 (2024) 10246–10250.
[5] H. Kono, Y. Li, R. Zanasi, et al., J. Am. Chem. Soc. 145 (2023) 8939–8946.
[6] Z.T. Li, X.D. Hou, Y. Han, et al., Angew. Chem. Int. Ed. 61 (2022) e202210697.
[7] A. Mishra, C.Q. Ma, P. Bäuerle, Chem. Rev. 109 (2009) 1141–1276.
[8] H. Miyoshi, S. Nobusue, A. Shimizu, Y. Tobe, Chem. Soc. Rev. 44 (2015) 6560–6577.
[9] M. Stępień, E. Gońka, M. Żyła, N. Sprutta, Chem. Rev. 117 (2016) 3479–3716.
[10] A. Borissov, Y.K. Maurya, L. Moshniaha, et al., Chem. Rev. 122 (2022) 565–788.
[11] R. Jasti, J. Vhattacharjee, J.B. Neaton, C.R. Bertozzi, J. Am. Chem. Soc. 130 (2008) 17646–17647.
[12] A. Stergiou, J. Rio, J.H. Griwatz, et al., Angew. Chem. 131 (2019) 17909–17914.
[13] Y. Yang, O. Blacque, S. Sato, M. Juríček, Angew. Chem. Int. Ed. 60 (2021) 13529–13535.
[14] K. Li, Z. Xu, H. Deng, et al., Angew. Chem. Int. Ed. 60 (2021) 7649–7653.
[15] J.P. Mora-Fuentes, M.D. Codesal, M. Reale, et al., Angew. Chem. Int. Ed. 62 (2023) e202301356.
[16] J. Krömer, I. Rios-Carreras, G. Fuhrmann, et al., Angew. Chem. Int. Ed. 39 (2000) 3481–3486.
[17] G. Fuhrmann, T. Debaerdemaeker, P. Bäuerle, Chem. Commun. 8 (2003) 948–949.
[18] F. Zhang, G. Götz, H.D.F. Winkler, C.A. Schalley, P. Bäuerle, Angew. Chem. Int. Ed. 48 (2009) 6632–6635.
[19] F. Zhang, G. Götz, E. Mena-Osteritz, et al., Chem. Sci. 2 (2011) 781–784.
[20] E. Mena-Osteritz, P. Bäuerle, Adv. Mater. 13 (2001) 243–246.
[21] G. Fuhrmann, J. Krömer, P. Bäuerle, Synth. Met. 119 (2001) 125–126.
[22] M. Bednarz, P. Reineker, E. Mena-Osteritz, P. Bäuerle, J. Lumin. 110 (2004) 225–231.
[23] K. Bold, M. Stolte. K. Shoyama, et al., Angew. Chem. Int. Ed. 61 (2022) e202113598.
[24] S.D. Veer, V.C. Wakchaure. K. Asokan, et al., Angew. Chem. Int. Ed. 62 (2022) e202212934.
[25] X. Zhang, H. Liu, G. Zhuang, S. Yang, P. Du, Nat. Commun. 13 (2022) 3543–3552.
[26] T. Zhou, R. Hu, L. Wang, et al., Angew. Chem. Int. Ed. 59 (2020) 9952–9956.
[27] H. Li, H. Wen, Z. Zhang, et al., Angew. Chem. Int. Ed. 59 (2020) 20371–20375.
[28] K.N. Wang, L.Y. Liu, D. Mao, et al., Angew. Chem. Int. Ed. 61 (2022) e202114600.
[29] Y. Wang, Y. Zhang, J. Wang, X.J. Liang, Adv. Drug Deliv. Rev. 143 (2019) 161–176.
[30] Y.N. Hong, J.W.Y. Lam, B.Z. Tang, Chem. Soc. Rev. 40 (2011) 5361–5388.
[31] Q. Peng, Z.G. Shuai, Aggregate 2 (2021) e91.
[32] F. Würthner, T.E. Kaiser, C.R. Saha-Möller, Angew. Chem. Int. Ed. 50 (2011) 3376–3410.
[33] Z. Zhao, J.W.Y. Lam, B.Z. Tang, J. Mater. Chem. 22 (2012) 23726–23740.
[34] L. Wang, Z. Xiong, J.Z. Sun, et al., Angew. Chem. Int. Ed. 63 (2024) e202318245.
[35] Z. Xiong, J. Zhang, J.Z. Sun, H. Zhang, B.Z. Tang, J. Am. Chem. Soc. 145 (2023) 21104–21113.
[36] M. Lian, Y. Mu, Z. Ye, et al., Aggregate 5 (2024) e560.
[37] Y.Y. Li, Z.C. Cai, S.J. Liu, et al., Nat. Commun. 11 (2020) 1255.
[38] L.B. Ren, Y. Han, X.D. Hou, et al., CCS Chem. 6 (2024) 2758–2769.
[39] A. Rana, Y. Hong, T.Y. Gopalakrishna, et al., Angew. Chem. Int. Ed. 57 (2018) 12534–12537.
[40] L.W. Ma, C.P. Li, Q. Yan, et al., Chin. Chem. Lett. 31 (2020) 361–364.
[41] S.N. Lei, H. Cong, Chin. Chem. Lett. 33 (2022) 1493–1496.
[42] Q. Feng, N. Li, Z.Y. Zhang, et al., Chin. Chem. Lett. 34 (2023) 108439.
[43] T. Lu, F. Chen, J. Comput. Chem. 33 (2011) 580–592.
[44] A. Tarai, M.N. Huang, P. Das, et al., Molecules 25 (2020) 585–598.
[45] L. Yao, S.T. Zhang, R. Wang, et al., Angew. Chem. Int. Ed. 53 (2015) 2119–2123.
[46] F. Wang, X. Li, s. Wang, et al., Chin. Chem. Lett. 27 (2016) 1592–1596.
[47] Y.Q. Chen, Y. Wang, Y. Yuan, et al., Phys. Chem. Chem. Phys. 17 (2015) 1309–1316.
[48] L.J. Wang, Y.C. Zhang, X.D. Huang, et al., J. Mater. Chem. C 11 (2023) 9308–9315.
[49] T.X. Xiao, J. Wang, Y. Shen, et al., Chin. Chem. Lett. 32 (2021) 1377–1380.
[50] Z. Zhao, X.Y. Zheng, L.L. Du, et al., Nat. Commun. 10 (2019) 2952–2961.
[51] P.J. Zhang, Q.F. Shen, Y. Zhou, et al., Chin. Chem. Lett. 34 (2023) 107910.
[52] M. Liu, S.H. Zhong, B. Feng, et al., Chin. Chem. Lett. 34 (2023) 107940.
[53] Z.W. Guo, J. Zhao, Y.H. Liu, et al., Chin. Chem. Lett. 32 (2021) 1691–1695.
[54] X.H. Zhang, Y. Qin, H.C. Zhang, et al., Chin. Chem. Lett. 36 (2025) 110715.
[55] N.L.C. Leung, N. Xie, W. Yuan, et al., Chem. Eur. J. 20 (2014) 15349–15353.
[56] L. Xu, Z. Wang, R. Wang, L, et al., Angew. Chem. Int. Ed. 59 (2019) 9908–9913.
[57] H. Yang, J. Zheng, M. Xie, et al., ACS Mater. Lett. 4 (2022) 1921–1928.
[58] J. Luo, Z. Xie, J.W.Y. Lam, et al., Chem. Commun. 18 (2001) 1740–1741.